Revised Draft

Proceedings of the ASME 2020
Pressure Vessels & Piping Division Conference
PVP2020
July 19-24, 2020, Minneapolis, MN, USA

PVP2020-21077

RESIDUAL-STRESS, MATERIAL CHARACTERIZATION IN P22 HRSG-PIPELINE BUTT JOINT

Ottaviano Grisolia
INAIL, Central Research Directorate,
Department of Technology
Via R. Ferruzzi, 38-40 00143 Rome, Italy
Phone: +39 06 97896431
Email: o.grisolia@inail.it

Lorenzo Scano, Francesco Piccini
Studio Scano Associato,
Safety & Integrity
P. le Chiavris, 66 33100 Udine, Italy
Phone: +39 0432 479456
Email: lorenzo.scano@studio-scano.it;
Email: francesco.piccini@studio-scano.it

Antonietta Lo Conte
Politecnico di Milano,
Dipartimento di Meccanica
Via La Masa, 1 20100 Milan, Italy
Phone: +39 02 23998223
Email: antonietta.loconte@polimi.it

Massimiliano De Agostinis, Stefano Fini
Università di Bologna, DIN
V.le Risorgimento, 2 40136 Bologna, Italy
Phone: +39 051 2093455
Email: m.deagostinis@unibo.it;
Email: stefano.fini@unibo.it

ABSTRACT

Previous study evaluated residual stress in a circumferential "V"-groove butt joint of a heat-recovery steam generator (HRSG) pipeline; the material was ASTM A-335-Grade P22. Aim had been to check on the influence over creep-relaxation previously found out for a tee made of the same material. The butt joint had been operating for the same period of 200,000 hours, same temperature of 528°C at almost a half pressure (0.46 Kg/mm^2 vs. 1.06 Kg/mm^2). X-ray diffraction (XRD) technique applied close to the weld highlighted anomalously high stress-level on the outer surface for all four butt-joint samples tested. Residual-stress over 400 MPa observed along the cylinder's tangential direction was statically not acceptable. On the inner surface where deposited beads may have tempered adjacent base material, measurement via blind hole-drilling (BHD) technique showed a symmetrical plane-state residual-stress of 199 MPa. It was consistent with that observed via XRD on the outer surface in the cylinder's longitudinal direction. Supposing a case of incomplete post heating planned for the weld may have explained the occurrence of being much higher than 40 MPa, value predicted after 200,000 hours. Similar influence over creep results found out for the tee and the butt joint had validated modeling welding simulation considered for both joints. A comprehensive new series of XRD tests aims now at measuring residual stress across the cylinder's wall, both inner and outer sides. The shallow layer considered has thickness sufficient for building a map of measurements covering different depths and locations on the surface. The experimental plan includes also BHD tests supporting the XRD ones. Comparison with previous measurements roughly shows stress level increasing similarly across the cylinder's wall from the inner side on: Average stress values, however, appear lower than previous measurements, showing better compatibility to the analysis results.

Keywords: creep, weld, welding, testing.

NOMENCLATURE

BHD	Blind hole-drilling (technique)
d(-spacing)	Distance between adjacent crystalline planes
E	Young's modulus
FEM	Finite element analysis, model
FWHM	Full width at the half maximum height of the peak, as measure of the intensity to record
HAZ	Heat-affected zone
HRSG	Heat-recovery steam generator
INAIL	Istituto Nazionale di Assicurazione contro gli Infortuni sul Lavoro (Italy Insurance Agency against Work-related Risks)
{hkl}	Miller's indices describing a family of crystalline planes (211 for ferrite, α iron)
K-α_1	Wavelength of characteristic line K-α (most

	intense radiation) used in X-ray diffraction
K-β	Characteristic line to remove
MT	Magnetic test
m'	Gradient of d(-spacing) vs. $\sin^2 \psi$
OM	Optical microscope
PWHT	post weld heat treatment
R	Radius to the longitudinal center of the gage
R_0 , $R_{0\,act}$	Nominal, actual hole radius
SEM	Scansion electronic microscope
t	Time
XRD	X-ray diffraction (technique)
Z	Hole depth
α	Angle from the nearer principal axis to the first of the three gages
$\dot{\varepsilon}$	Creep strain rate
ε	Creep strain, rupture ductility
ε_c $\dot{\varepsilon}_c$	Critical value for creep strain, strain rate
ε_0 , σ_0	Initial values for creep strain, applied stress
λ	Wavelength of the X-ray
ν	Poisson's ratio
σ, σ_θ	Applied, membrane-tangential stress
σ_c	Critical value for relaxed stress
σ_{VM}	Von-Mises equivalent stress
σ_i	Principal stress, for i =1, 2, 3
σ_{min} , σ_{max}	Minimum, maximum principal stress
φ	Angle between a chosen direction in the sample's plane and the projection of the normal to the diffracting plane
ψ	Angle between normal to the sample and normal to the diffracting plane
ω	Angle of the goniometer in the scattering plane

INTRODUCTION

Worked case considered herein is the same as that considered for both thermal and creep analysis of previous study [1]: it is a 26-meters high-energy pipeline for deriving steam from HRSG to different technological plant. It operated at temperature of 528°C and pressure of 0.46 Kg/mm^2; manufactured from ASTM A 335-Grade P22, it had nominal outer-diameter of 406.4 mm and thickness of 21.44 mm. Fig. 1 shows both the pipeline layout and the weld cross-section scheme for the circumferential "V"-groove butt joint previously analyzed. Since pipeline's section including the joint was on the ground, sustained load condition for the weld was negligible. At operating condition, maximum equivalent-stress (maximum between hoop + sustained and hoop + thermal expansion) would be at the welded joint because of the intensification. There, residual stress because of weld cooling in the air produced in addition an initial peak of secondary stress (σ_{VM} = *215.29* MPa). Welding-process simulation for the circumferential butt joint considered areas most affected by possible metallurgical issues. The latter are hardening of the base metal and cracks in both weld and base metal, the latter independent of base's microstructure conditions. Therefore, thermal analysis covered the heat-affected zone (HAZ) next to the fusion line attaining the maximum hardness values, though grain growth at high temperature [1], [2]. FEM simulation, however, did not aim at evaluating microstructural change during welding.

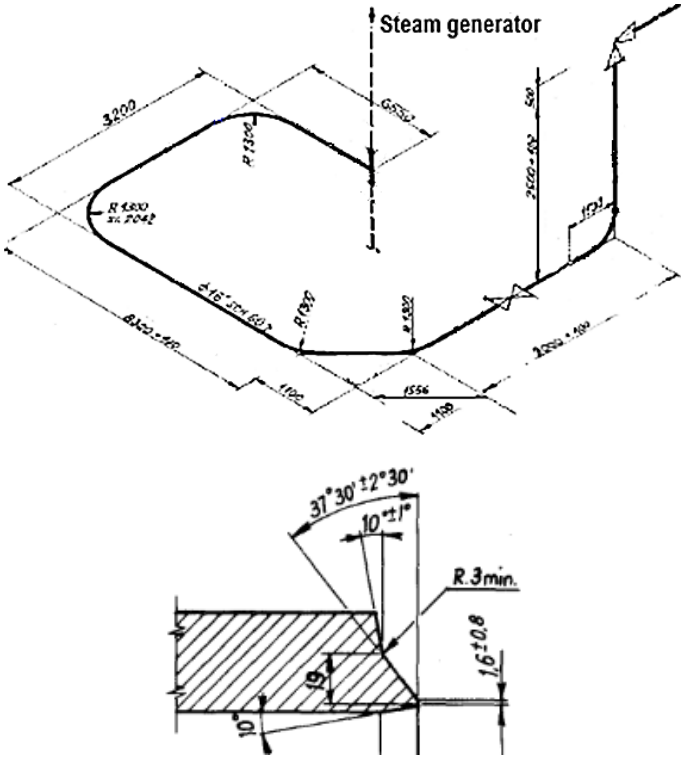

FIGURE 1. **[1]** HRSG PIPELINE LAYOUT, WELD CROSS-SECTION SCHEME FOR THE CIRCUMFERENTIAL BUTT JOINT

1. ANALYZING THE HRSG-PIPELINE [1]

1.1 Modeling Welding Process for Circumferential "V"-groove Butt-joint [1]

Process considered in the numerical simulation is string, multiple-pass with full-penetration. Data used come from the available manufacturer's documentation and from joint's section OM observation (Fig. 14). They included a 2% thoriated-tungsten single-electrode with De^ of 2.4 mm, d^ of 8 mm and maximum oscillation of 2°; current was of 80-120 A, voltage of 12-14 V DC and travel speed of 4.5 mm/sec. For each lay, simulation conservatively considers residual-stress distribution in both weld and base metal: this assumption would represent a worst-case scenario, also disregarding preheating the base metal and post heating or tempering. In so doing, both maximum Von-Mises and tangential stresses found out are those from either thermal load or the thermal gradient applied on the joint: model 3-D elements include both weld beads and adjacent base metal. This, being colder hinders weld-contraction: analysis assumes temperature's differential attained during cooling as the maximum thermal load between weld and base metal (boundary condition). For the weld pool, temperature assumed initially is 1400°C (average melting point for P22 [13]); for the adjacent base metal, it is that predicted by thermal analysis, T. Final temperature is 22°C (room). Maximum plane-state stress (hot shrinkage) found out in the transitory is that from the thermal gradient applied on bead's model 3-D elements: the maximum rate considered is (1400 – 22) [°C] / $t_{w\ cooling}$ [hours]. Maximum stresses found out in the adjacent base metal during the transitory, are from base metal's different contraction: the maximum rate considered is (T – 22) [°C] / $t_{b\ cooling}$ [hours]. Conservative assumption of disregarding

pre and post heating should balance that of not considering any bead's cross-section reduction and base's higher hardness. Analysis assumes a temperature-based approach in modeling the gas-tungsten arc-process. Commercial software used (Ansys release 19.01) features element-birth and death technique to simulate beads' deposition by electrode traveling through the welding process. Table 1 recaps data used for modeling welding process in butt-joint thermal analysis.

TABLE 1. DATA USED IN MODELING WELDING PROCESS FOR BUTT-JOINT THERMAL ANALYSIS **[1]**

Welding Process	**Multiple-pass, Full-penetration**	***Note***
Weld's cooling initial temperature [°C]	1400	^
Base's cooling initial temperature [°C]	723	^
Cooling final temperature [°C]	22	*room*
$\dot{q}_V$ [W/m^3]	-	*
$\dot{q}_S$ [W/m^2]	-	*
c_p [J/Kg °K]	-	‘
k [W/m °K)	-	‘
h [W/mm^2 °C]	1.5E-5	^
e **[7]**	0.2	^
ρ [Kg/m^3]	7850	^
Electrode's travel speed [mm/sec]	4.5	^
^Value coming from literature		
**Not an input since temperatures introduced in the model*		
‘Value dependent on temperature, as in References [7], [9]		

1.2 FEM Thermal-Analysis for “V”-groove Butt-joint[1]

In the analysis, (Fourier law) conservation of energy-derived heat-equation governs relation T(x, y, z, t) as follows [10]:

$$\rho c_p \frac{\partial T}{\partial t} - k \frac{\partial^2 T}{\partial n^2} = \dot{q}_V \quad (1)$$

The above equation applies to each 3-D element (body), subject to a volumetric heat source $\dot{q}_V$ (a flow rate of heat energy per unit volume). Across the body's surface, heat-equation expresses the boundary condition as follows:

$$\rho c_p \frac{\partial T}{\partial t} - k \frac{\partial^2 T}{\partial x^2} = \dot{q}_S = h(T - T_s) + 5.67E-8\, e(T^4 - T_s^4) \quad (2)$$

In the latter equation, $\dot{q}_S$ is the flow rate of heat energy per unit area; h and e are the convection and emissivity coefficient respectively; T and T_s are the body's surface temperature and surrounding temperature respectively. In both equations, t and ρ are time and the mass density of material respectively; c_p and k are the specific heat capacity and the thermal conductivity along n, x-direction respectively. Stress-strain diagrams for P22 (assumed isotropic) showing hardening behavior are in [7], [9].

1.3 FEM Thermal and Creep Analysis Results [1]

Up to 10 hours, realistic stress-dependency was that in Fig. A1 in the Annex A (thermal analysis, residual stress) since welding carried out without pressure at room temperature. At the end cooling, stresses reduced instantaneously because of discontinuity (the longitudinal from over ±250 MPa to ±70 Mpa); afterward they relaxed during operation to a minimum after 200,000 hours (the equivalent reaching *40* MPa). Fig. A2 shows residual-stress distribution (equivalent, longitudinal and the hoop) attained on the weld after ten hours (end cooling). Maximum σ_{VM} was of *256.15* MPa on the outer surface, 50 mm from the weld. Both longitudinal and hoop stresses attained maximum value at 50 mm from the weld on the inner surface. During operation, pressure and temperature contribution produced the stress-dependency over time shown in Fig. A3. Fig. A4 shows maximum equivalent stress and creep-strain obtained with and without residual stress contribution (using same Norton coefficients [4], [5], and [6]). With an initial predominance of the former case's results, tendencies converged to a common value after 200,000 hours. Fig. A5 shows stress distribution after 10 and after 200,000 hours of operation.

2. EXPERIMENTAL ACTIVITY

2.1 Using Two Methods Simultaneously

Both XRD and BHD techniques measure strain within limited distance from the sample surface: thus, values of related stress obtained may be comparable assumed the applicability of both methods. This mainly depends on how test material is far from being homogeneous, isotropic and linear-elastic. Ultimately, this is the necessary condition for use of equations expressing stress as the principal one in both techniques. XRD expresses stress in the surface's direction φ in terms of principal stress σi and modulus of elasticity E. BHD expresses the relieved stress in terms of relieved radial and tangential strain, the former in terms of principal-stress, (nearer principal-axis) direction and (material) coefficients. Thus, minimum and maximum stress and direction are as a function of (the principal axis) relieved-strain.

2.2 Test Material, Samples and Specimens

Test material consists of the HRSG pipeline's section shown in Fig. 2 including the joint in the centerline. Manufactured in 1976 from ASTM A 335-Grade P22, the section has length of about the pipeline's nominal outer-diameter. From the manufacturer's available documentation, there should have been pre heating at 250°C; the post weld heat-treatment (PWHT) should have included the following: tempering (three hours at 680-720°C), annealing (700-720°C) with cooling in the air and normalizing (30 minutes at 950-980°C). The previous test plan [1] included withdrawal of four samples (small, 1, 2 and 3). For technical reasons, XRD application was on the outer surface (all samples), BHD application was on the inner surface (the sample 1). All samples consisted of the cylinder's longitudinal-section, the width of about six times the thickness. This dimension proved to be sufficiently safe for the effectiveness of measurements, which returned minimum residual stress at 50 mm from the fusion line. Fig. 2 shows samples (small and 1) used again for present study with both test and specimen-withdrawal locations sketched on their surface. The small sample used for preliminary measurements provided the three specimens shown in Fig. 3: specimen 1 (above) was for the OM observation; specimen 2 and 3 were for the SEM. Figures 4 and 6 show previously observed creep-damage and joint morphology, respectively. Surface preparation always included cleansing, degreasing and oxidation removal by solvent from area of measurement. For BHD, it included also fine grinding.

2.3 Test Material Examination

Presently, further metallographic methods and the OM observation have helped understand whether and how the base material is far from being homogeneous, isotropic and linear-elastic. This point is important for checking on both material's behavior and methods' applicability. Visual check and the MT have detected on pipeline's surface longitudinal flaws, maximum length and depth of 90 mm and <1 mm respectively. Fig. 5 shows cracks detected through MT and OM observation by Breda, seat of Cormano, Italy [7]. Possibly caused by material particles folding beneath the surface during hot working (forging and/or rolling), they may affect microstructure of adjacent base metal. High temperature may promote reduction of iron (Fe) oxide with aluminum (Al) and silicon (Si) through the two following chemical reactions respectively [7] [8]:

$$2Al + 3FeO \rightarrow Al_2O_3 + 3Fe; \quad Si + 2FeO \rightarrow SiO_2 + 2Fe \qquad (3)$$

After both globular Al and Si oxides have taken place in the microstructure close to the cracks, carbides begin to disappear through the following chemical reaction:

$$C + FeO \rightarrow CO + Fe \qquad (4)$$

The presence of both oxides formed at carbides' expense inside the outer layer's microstructure may be the principal cause of XRD results' dispersion.

2.4 Residual Stress Measurements

The present test plan has included material removal from samples' surface by electrolytic method to reach the desired depth. Table 1 recaps method's parameters. Incremental material removals have been of .05 and .10 mm over the test area. XRD tests have been at 5, 20, 50 mm from the weld; BHD tests have been at 20 mm, which was the reference location in previous study. Techniques' application has been on both sides of each sample, specifically of the small one for XRD and of 1 for BHD. Fig. 2 shows both samples used for the present activity.

TABLE 2. ELECTROLYTIC-REMOVAL PARAMETERS

Reagents applied	94% acetic acid, 6% perchloric acid
Tool	Movipol 3
Current [A]	0.2 - 0.5
Voltage [V]	75
Number of applications	4 or 5 or 7 (per each location)
Depth [mm]	0.5 or 0.10 (per single removal)

2.5 Measuring Residual Stresses via XRD

Tables 2 and 3 summarize main parameters for the lab's diffractometer and for stress calculation [1] respectively. Stress measurements carried out at the university lab's facilities in Milan, should comply with the good practice guide and standardization of References [10] and [11].

TABLE 3. MEASUREMENT PARAMETERS (XRD)

Diffractometer	X stress 3000
Manufacturer	AST Stress tech
X-Ray tube	Cr
Collimator Ø [mm]	1, 2
Filters	K-β
Exposition time [sec]	30
Calibration material	α-ferrite
Diffraction peak θ [°]	156.1
Wavelength [Å]	2.2897
Cristallographic plane	{211}

TABLE 4. STRESS-CALCULATION PARAMETERS (XRD)

Tube current [mA]	6.7
Tube voltage [kV]	30
Tilt geometry	Ψ
Number of inclinations	4/4
Angle of inclination [°]	+/- 45
Φ, Ψ Oscillation	0
Young's module E [Mpa]	211000
Poisson's ratio ν	0.33
Stress formula [1]	E/(1+ν) m'

2.6 Discussing XRD Measurements

Table A1 gathers stresses observed on the small sample's outer and inner surface, in the cylinder's longitudinal axis (90°) and the other two directions (0°, 45°). Distances from the weld have been 5, 20 and 50 mm. Stresses observed in 0° and 90° -direction show good consistency with the principal stresses. Consistency appears to worsen using a 2-mm collimator as an attempt at the maximum depths only: generally, stresses appear to decrease and the principal ones increase (bold blue values). Stresses observed on the outer surface (bold red values) though lower than previous of Table A2 (bold values) are still not consistent with the pipeline's long service (200,000 hours). They are also statically unacceptable, being much higher than pressure-case membrane tangential-stress ($\sigma_\theta = 42.183$ MPa) [1]. Stress level lowers dramatically on the inner surface/side being consistent with value of 40 MPa predicted by creep analysis: it parallels the difference between stresses on the outer and inner surface previously found out (though via different techniques). The circumstance appears now extended to layer below the surfaces, somehow confirming the distribution across the cylinder's wall previously assumed [1]. Stress appears increasing through the pipeline's thickness from the inner side on. On the other hand, comparison with stresses previously observed at the reference station (20 mm from the weld, 90° direction) [1] says this: Average stress level through .30 mm-layer is 80 MPa on the outer side and 43 MPa on the inner side. They base on the stress values of Table A1 (bold orange), their absolute values shown graphically in Fig. 8. These two absolute stress values compare to the average stress level of 110 MPa previously observed on the outer surface. It bases on the two stress values of Table A2 (bold orange) observed specifically on the sample 1 and 2.

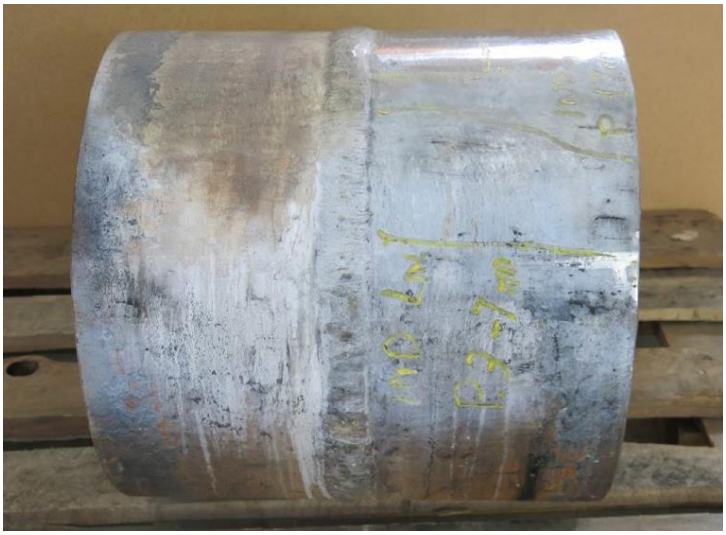

FIGURE 2. PIPELINE'S TEST SECTION (ABOVE); SMALL SAMPLE SHOWING ON TWO MARGINS' OUTER SURFACE SPECIMEN WITHDRAWAL ZONES; SAMPLE 1 SHOWING ON THE INNER SURFACE BHD LOCATION (20 MM FROM THE WELD) **[1]**

FIGURE 3. SPECIMEN 1 PREPARED FOR OM OBSERVATION AND SPECIMENS 2, 3 PREPARED FOR SEM (BELOW) **[1]**

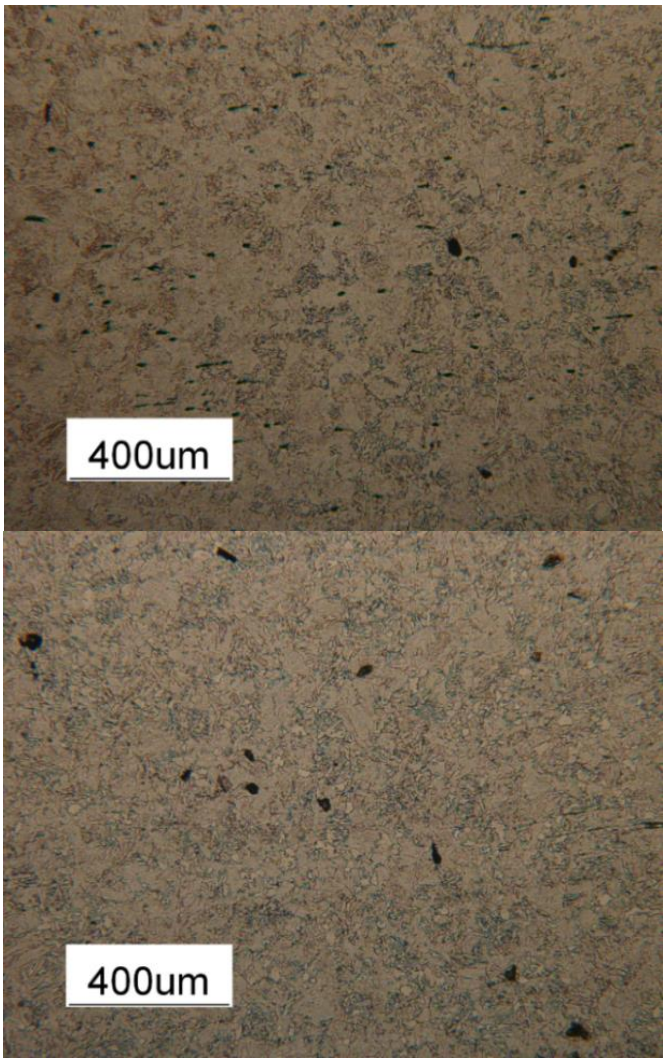

FIGURE 4. ORIENTED CAVITATIONS PREVIOUSLY DETECTED BY THE SEM ON THE WELD (ABOVE) AND HAZ: P22 AFTER 200,000 HOURS OF OPERATION AT 528°C **[1]**

FIGURE 6. BUTT-JOINT WELD'S MORPHOLOGY (THREE LAY, THE THIRD OF FOUR PASSES) PREVIOSLY OBSERVED BY THE OM **[1]**

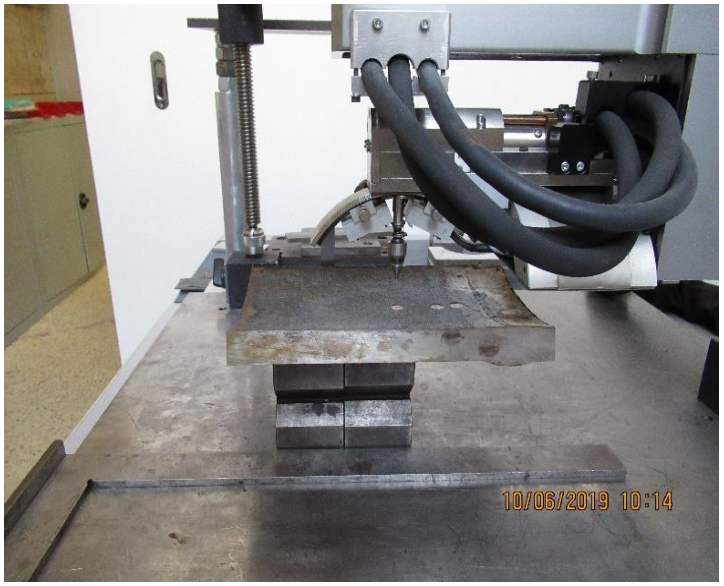

FIGURE 5. PIPELINE'S SURFACE LONGITUDINAL CRACKS DETECTED BY THE MT (ABOVE), OM OBSERVATION (COURTESY OF BREDA, CORMANO SEAT, ITALY) **[7]**

FIGURE 7. THE SAMPLE (SMALL) INTO DIFFRACTOMETER LAB'S ENCLOSURE FOR XRD STRESS MEASURMENTS

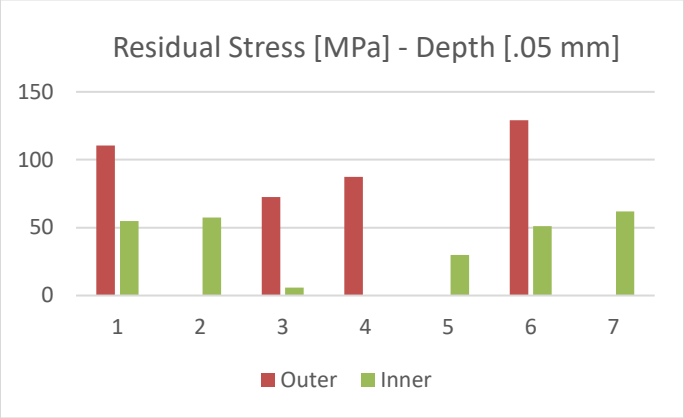

FIGURE 8. STRESS LEVEL OBSERVED THROUGH 0.30 MM LEYER ON BOTH SIDES OF THE SMALL SAMPLE; XRD TECHNIQUE APPLIED AT 20 MM FROM THE WELD

Lacking further experimental data, present study still considers the assumption of possible defective post heating the base metal (tempering) and incomplete PWHT (annealing) hindering creep relaxation. Consequences on creep behavior may have been especially for the piping's outer side where the welding tempering effect is lower. Stress uncertainty generally much higher than 10% shows now a data dispersion justifiable through the microstructure changes described in Par. 1.3. In the outer layer, they accompany the flaws detected by MT and OM and shown in Fig. 5. Chemical analysis and metallographic tests carried out by Breda say that base material gradually regains its standard properties away from the surface. Table 4 includes the element's contents observed by spectrograph, compared to P22 ASTM-Specification [7] [9]: all values appear within standard ranges.

TABLE 5. CHEMICAL COMPOSITION OBSERVED VS. STANDARD: P22 AFTER 200,000 HOURS OF OPERATION AT 528°C (COURTESY OF BREDA, CORMANO SEAT, IT) **[7]**

	C	Si	Mn	P	S	Cr	Mo	Ni	Cu
Obs.	13	.33	.45	.007	.018	2.44	1.04	.15	.15
Std. [9]	.05 ÷ .15	< .5	.3 ÷ .6	< .025	< .025	1.9 ÷ 2.6	.87 ÷ 1.13	-	-

Breda carried out also hardness measurements for two different sections of pipeline: average hardness values are 146 HV and 165 HV respectively, observed applying 1 Kg 15 sec (five measurements) [7]. They compare to 138 HV, ASTM-Specification average value for P22 [9]. Hardness higher than standard values may suggest lower tempering temperatures. This because customarily, process tempering should reduce hardness by coarsening carbide precipitate. Higher strength also attained consequently may justify high stresses observed on the outer surface. Except the surface, based on Breda test results, base material may be ideal enough for the applicability of both stress-measurement methods. Now, one may consider the reference station at 20 mm from the weld: Table 5 gathers stresses previously predicted after 10 hours (end-cooling) and 200,000 hours (operation), according to Figures A2 and A5 respectively; it gathers also the average of stresses presently observed via XRD through .30 mm-layer on the small sample' both sides. The latter are highlighted bold orange in Table 6. This table includes angle φ, FWHM of the peak and software errors: the latter base on the statistical estimate in the plot d vs. $\sin^2\psi$. The diffraction peak intensity is similar at different tilts, indicative of a not highly textured material.

TABLE 6. RESIDUAL STRESS PREDICTED AND AVERAGE OBSERVED VIA XRD THROUGH THE LAYER, 20 MM FROM THE WELD, THE OUTER AND INNER SIDE

Period [Hours]	10		200,000	200,000	
Sample's side	Outer	Inner	Out./Inn.	Outer	Inner
Stress [MPa]	Predicted			Observed	
Longitudinal	-270	240		32	23
Hoop	-125	25		**120**	35
Equivalent	256		40		

Comparison of stresses predicted at 10 and 200,000 hours (Figures A2, A5 respectively) with the average observed through the layer (bold orange values of Table A1) says this: On the inner side, both longitudinal and hoop stresses predicted at the end cooling and both observed (after relaxation) appear tensile. The latter are consistent with the equivalent predicted after relaxation (40 MPa). On the outer side, both predicted stresses appear compressive while both observed ones appear tensile. The longitudinal observed is consistent with the equivalent predicted after relaxation. Instead the hoop appears as important as the predicted at the end cooling (-125 MPa) with the sign inverted. After 200,000 hours of operation, on the outer side, observed hoop residual-stress appears tensile and unrelaxed: it is 120 MPa, highlighted bold in Table 5 (vs. 35 MPa on the inner side). This may be the consequence of defective tempering followed by incomplete annealing: Customarily, both treatments, raising temperature some degrees (centigrade) below and few tens above the transformation range respectively, should obtain relief of internal stresses [3]. Keeping tempering temperature lower may have hindered inversion of the hoop stress on the outer surface, predicted as compressive by thermal analysis.

Though circumstance not experimentally proved, incomplete annealing may have caused insufficient carbon distribution into austenite: this may have had influence over material's ductility and thus on creep relaxation. Fig. 9 schematically shows creep damage and rupture-ductility over stress relaxation, as observed in creep or creep-fatigue tests (long hold-time) [12] [13] [14]. Under high stress levels, creep strain is a consequence of matrix deformation with larger elongation and area reduction at rupture. Under low stress levels, the latter are smaller since creep damage mainly coming from the cavitations at grain boundaries. Fig. A4, shows both stress relaxation and strain tendencies as previously predicted by the creep analysis (red lines) for the butt-joint. Supposing similar damage types over creep range, most of the cavitations previously detected (Fig. 4) should relate to the pipeline's inner side: this portion exhibits lower observed residual stress.

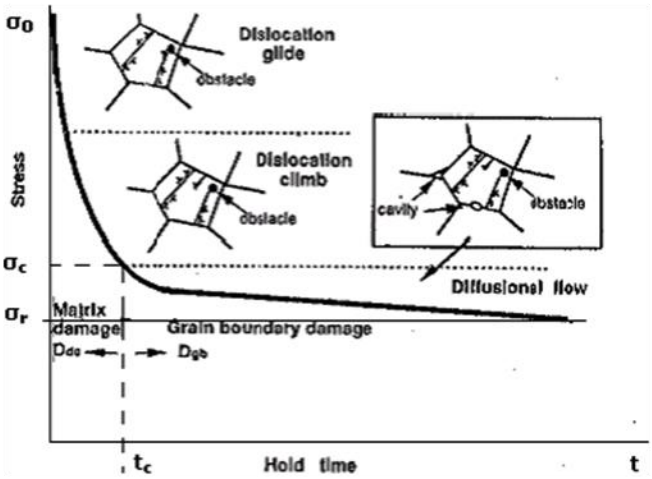

(COURTESY OF EMAS PUBLISHING, **[12], [14])**

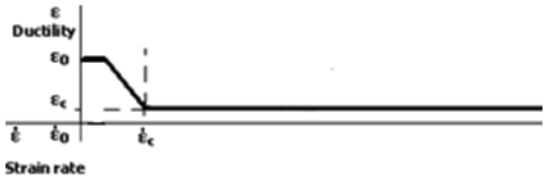

(REPRINTED WITH PERMISSION OF ASM INTERNATIONAL. ALL RIGHTS RESERVED. WWW.ASMINTERNATIONAL.ORG **[13], [14]**)

FIGURE 9. CREEP DAMAGE AND DUCTILITY (BELOW) OVER STRESS RELAXATION: CREEP TESTS OR (LONG) HOLD-TIME CREEP-FATIGUE TESTS **[14]**

2.7 Measuring Residual Stresses via BHD

Table 7 summarizes main parameters for stress calculation [1].

TABLE 8. MEASUREMENT PARAMETERS (BHD)

Precision milling-guide	RS200-Vishay
Milling-tool max speed [rpm]	400,000
Strain-gage rosettes	CEA-06-062UL-120
Resistance [Ohm]	120 ± 0.4%
Acquisition system	National Instruments
Carrier	Ethernet NI9184
Extensimeter module	NI9237
R, R_0 , $R_{0\,act}$ [mm]	2.5, 0.75, 0.98
Increment, max depth [mm]	0.05, 2
Residual-stresses calculation from measured relaxed-strains	Previously-developed PC program for Windows

Stress measurements carried out at the university lab's facilities, should comply with the good practice guide and standardization of References [15] and [16]. Fig. 10 is the scheme of strain gage rosettes arranged to measure residual stresses: gage grid 1 is along the cylinder's tangential direction x. Fig. 10 shows rosette installation at stations 7 and 8, 20 mm from the weld on the outer, inner surface respectively. Stations' numerals follow measurements carried out so far on the sample 1 in previous [1] and present experimental activity.

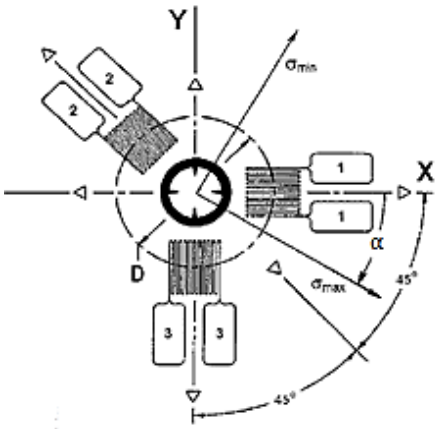

FIGURE 10. STRAIN GAGE ROSETTE ARRANGEMENT

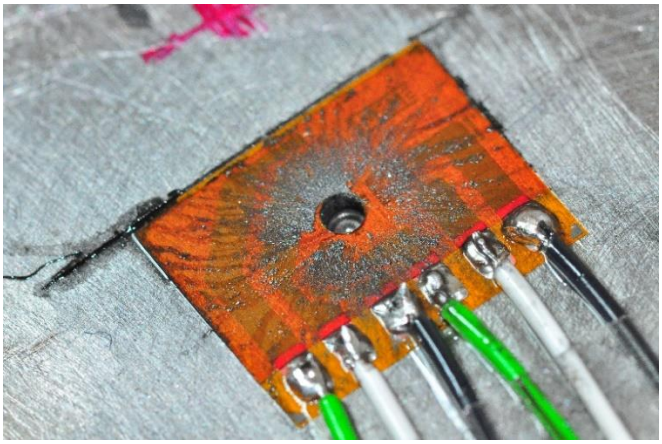

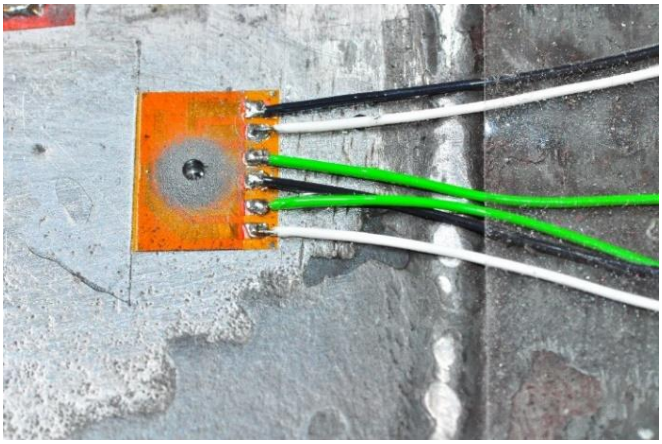

FIGURE 11. STATION-7 ROSETTE (THE OUTER SURFACE) AND STATION-8 ROSETTE (THE INNER SURFACE, BELOW)

2.8 Discussing BHD Measurements

Out of four measurements presently executed, two have returned acceptable results: they are those at stations 7 and 8 of Fig 11. Previuos experimental activity included same number of measurements executed and discarded. Fig. 12 shows check on regularity of the experimental fit (strain% - Z/D), which should have been within ASTM D837 fits (bold and dashed). Discarded measurements (stations 5 and 6) showed fit irregularity, caused by obstacles to the drilling damaging the milling tool. Microstructure changes found out

in the surface layer may explain these difficulties in the execution, similar to those found previously. Table 8 gathers the orientation, maximum and minimum stress observed on sample 1 (the outer surface, bold). On the sample's both surfaces, equivalent stress observed (31.22 MPa and 46.36 MPa respectively) is consistent with that predicted by creep analysis at 200,000 hours (40 MPa). Still, the difference between the two BHD measurements confirms the stress increase through the pipeline's thickness showed by XRD technique.

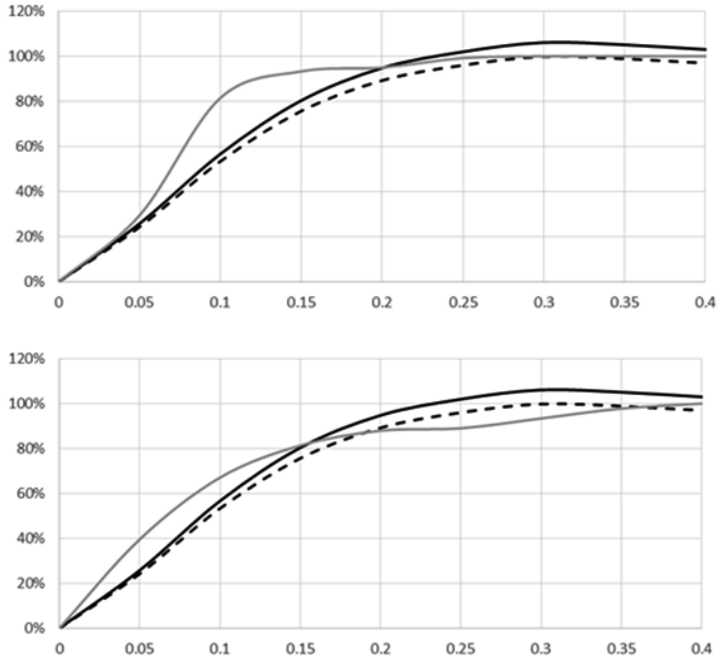

FIGURE 12. RELIEVED STRAIN % VS. Z/D: STATION 7 (OUTER SURFACE), STATION 8 (INNER SURFACE, BELOW)

TABLE 8. RESIDUAL STRESS, DIRECTION OBSERVED VIA BHD ON THE SAMPLE 1'S OUTER AND INNER SURFACE

Distance from the weld [mm]			20
Stress orientation [deg]		α (outer, inner)	**11.96** 1.75
Stress [MPa]	**Outer**	σ_{min} σ_{max}	**37** **52**
	Inner	σ_{min} σ_{max}	25 35

CONCLUSIONS

Primary study's goal has been to look into reasons for disparities between observed and predicted residual-stress values highlighted by previous characterization. Samples have been from the ASTM A-335-Grade P22 pipeline including the circumferential "V"-groove butt joint. Specifically, on the outer surface, maximum hoop stress previously observed via XRD was statically not acceptable for material's standard strength values; on the inner surface, symmetrical plane-state stress previously observed via BHD was much higher than predicted at 200,000 hours (relaxed value). Based on present hardness measurements, lower tempering temperature may have produced the higher strength values justifying the high hoop stresses observed on piping's outer surface. Presently, the experimental plan has included residual-stress measurements via XRD at three different locations, on both cylinder's surfaces; they have been through .25 mm-layer, with incremental material removals of .05 mm. Both tangential and longitudinal stresses observed at the reference station (20 mm from the weld) appear increasing through the pipeline's thickness from the inner side on. In particular, average longitudinal stress observed through the layer on both sides (43 and 80 MPa respectively) appears to confirm this; average value previously observed on the outer surface between two samples was of 110 MPa. BHD measurements show similar stress difference between the inner and outer surface, though equivalent-stress more consistent with value predicted at 200,000 hours. Predicted stresses from previous thermal and creep analysis and the average ones presently observed via XRD through the layer have provided a check on PWHT effectiveness. On the inner side, both longitudinal and hoop stresses observed appear tensile, as both stresses predicted at the end cooling. The observed are consistent with the equivalent predicted after relaxation. On the outer side, longitudinal stress observed is consistent with the equivalent predicted after relaxation; hoop stress observed appears nearly the same as the predicted at the end cooling except the sign inverted: after 200,000 hours of operation it appears still tensile and unrelaxed (120 MPa vs. 35 MPa on the inner side). Lower tempering temperature may have caused the former circumstance. Shorter annealing time instead may have influenced material's rupture ductility leading to lesser creep-relaxation on the pipeline's outer side. Creep-test relaxation applied to the butt-joint case may suggest that most of the cavitations previously detected should be at the pipeline's inner side, with lower observed residual stress.

Secondary study's goal has been to check on samples conditions, providing better characterization of test material. It has been mainly to probe into reasons for stress data dispersion in XRD measurements, with uncertainty higher than 10%: microstructure changes, observed by OM in the outer layer accompanying the longitudinal flaws detected by MT, may justify it. In BHD measurements, they may also explain residual-stress variability across the pipeline's surface and/or irregularity in the executions. Chemical analysis confirms standard properties of base material, gradually regained away from the surface: it somehow validates measurement methods' applicability.

ACKNOWLEDGEMENTS

Authors thank the colleagues Cristiano Bolgiani of EDISON, Milan, Italy and Luca Casiraghi of BREDA, Cormano, Italy for kindly allowing use of test-material experimental data. They also thank EMAS Publishing and ASM International for kind permission to image reprinting.

REFERENCES

[1] Grisolia O., Scano L. et Al., 2019," HRSG-pipeline Weld Residual-stress Measurement to Assess Influence over Creep-analysis Results from Italian Code, American Standard," PVP2019-93429 Proceeding of ASME Pressure Vessels & Piping Division Conference, San Antonio, TX

[2] Grisolia O., Scano L., 2018,"HRSG Header Welds Residual-stress Evaluation and Creep-Assessment through the Application of Italian Code, American Standard," PVP2018-84662 Proceeding of ASME Pressure Vessels & Piping Division Conference, Prague, Czech Republic
[3] Jefferson T.B., 1990, "Metals and How to Weld Them," The J. F. Lincoln Arc Welding Foundation, Cleveland, OH
[4] NIMS Testing Division, 1986, "Data Sheets on the Elevated-Temperature Properties of 2.25Cr-1Mo Steel For Boiler and Heat Exchanger Seamless Tubes (STBA 24)", 3B, National Research Institute for Metals
[5] Grisolia O., 2010, "Assessment of Weld Reduction Factors through Experimental Reference Curves," Engineering Fracture Mechanics. 77 2971-2991, Elsevier Ltd., Oxford
[6] Scano L., Esposito L., 2017,"Effect of Secondary Creep Formulation on API-579-1 Residual Life Evaluation," PVP2017-65512 Proceeding of ASME Pressure Vessels & Piping Division Conference, Waikoloa, HI
[7] BREDA, 2018, "Failure Analysis for P22 HRSG Pipeline," Technical Report N° 113, Cormano (MI), Italy (Issued in Italian)
[8] Cibaldi C., 1990, "Criteria for Steels and Pre, Post Heating Selection," Analisi Publishing, Italy (Issued in Italian)
[9] ASTM, 2007, A956-96 Standard Specification for Seamless Ferritic Alloy-Steel Pipe for High-Temperature Service
[10] M. E. Fitzpatrick at Al., 2005, "Measurement Good Practice Guide No. 52 – Determination of Residual Stress by X-ray Diffraction", National Physical Laboratory, UK
[11] EN 15305, 2008, "Non-destructive Testing - Test Method for Residual Stress analysis by X-ray Diffraction"
[12] Nitta A, Ogata A., 1995, "Life Assessment of High Temperature Components," Proceeding of "Materials Ageing and Component Life Extension" International Conference," 10-13 October, Milan, I, EMAS Publishing
[13] Viswanathan R., 1989, "Damage Mechanism and Life Assessment of High-Temperature Components," ASM International
[14] Grisolia O., 2013, "Analysis and Life Evaluation of High-temperature Pressure Equipment," Inail Publishing, Italy, (Issued in Italian, in print and on site digital version)
15] VISHAY Micro-measurements, 2007, "Measurement of Residual Stresses by the Hole-Drilling Strain Gage Method", Tech Note TN-503-6
[16] ASTM, 2007, Standard E 837, "Determining Residual Method", Tech Note TN-503-6

ANNEX A

TABLE A1. RESIDUAL STRESS OBSERVED VIA XRD ON THE SMALL SAMPLE'S OUTER AND INNER SIDE: PROGRESSIVE ELECTROLYTIC REMOVAL

P22 pipeline's small sample		Stress-mesurement direction							
		0° (cylinder's tangential direction)				**45°**			
Distance from the weld [mm], Location on the pipeline	Depth [mm]	**Stress** [Mpa]	Error (+-) [Mpa]	FWHM [°]	Error (+-) [°]	**Stress** [Mpa]	Error (+-) [Mpa]	FWHM [°]	Error (+-) [°]
5, Outer **surface**	/	**368.5**	6.2	2.05	0.04	**346.4**	12.1	2.04	0.06
5, Outer **side**	0.10	**231.0**	73.7	1.65	0.19	**17.9**	76.5	1.33	0.28
"	0.15	**393.5**	119.1	1.46	0.22	**358.3**	107.0	1.32	0.21
"	0.20	**76.3**	73.4	1.58	0.16	**130.4**	67.9	1.29	0.26
"	0.25	**133.7**	71.8	1.43	0.27	**222.8**	69.6	1.52	0.15
20, Outer **surface**	/	**249.3**	19.0	1.97	0.09	**238.8**	20.5	1.94	0.03
20, Outer **side**	0.10	**173.3**	117.1	1.35	0.36	**318.9**	231.6	1.24	0.35
"	0.15	**121.5**	69.7	1.14	0.18	**84.6**	140.5	1.47	0.46
"	0.20	**58.3**	96.4	1.44	0.22	**-0.9**	153.4	1.44	0.28
"	0.25	**119.5**	62.9	1.31	0.26	**257.0**	309.7	1.30	0.31
50, Outer **surface**	/	**209.9**	64.4	1.89	0.20	**133.2**	50.2	1.76	0.08
50, Outer **side**	0.05	**79.4**	43.9	1.61	0.18	**113.5**	78.7	1.55	0.15
"	0.10	**178.9**	55.8	1.61	0.12	**-23.8**	68.4	1.50	0.39
"	0.15	**-69.3**	109.6	1.32	0.33	**153.4**	79.5	1.27	0.12
"	0.25	**39.3**	150.7	1.29	0.24	**195.9**	97.3	1.41	0.18
"	0.30	**-121.8**	114.9	1.37	0.31	**147.5**	11.6	0.92	0.14
"	0.35	**-31.2**	85.0	1.37	0.19	**133.7**	150.1	1.28	0.30
"	0.40	**-94.4**	91.2	1.30	0.22	**-11.8**	77.4	1.13	0.36
5, Inner **surface**	/	**-14.8**	16.3	1.53	0.16	**-29.3**	27.5	1.43	0.13
5, Inner **side**	0.05	**-15.1**	42.8	1.50	0.15	**117.1**	61.5	1.45	0.24
"	0.10	**29.8**	32.4	1.57	0.22	**15.3**	50.5	1.37	0.21
"	0.20	**81.6**	43.5	1.25	0.20	**12.9**	51.0	1.30	0.27
"	0.30	**28.6**	56.5	1.49	0.13	**-24.6**	32.0	1.42	0.17
"	0.35	**-39.4**	28.5	1.37	0.28	**141.8**	42.5	1.34	0.23
"	0.35	**-137.2**	31.9	1.58	0.15	**107.6**	54.8	1.67	0.10
20, Inner **surface**	/	**-0.8**	85.6	1.34	0.30	**-52.2**	15.8	1.46	0.16
20, Inner **side**	0.05	**-2.3**	35.3	1.35	0.19	**77.1**	23.2	1.33	0.21
"	0.10	**-11.5**	24.2	1.59	0.10	**117.5**	21.6	1.39	0.14
"	0.20	**40.7**	47.5	1.41	0.13	**77.9**	40.0	1.38	0.21
"	0.25	**56.4**	55.4	1.39	0.14	**-34.3**	44.1	1.41	0.20
"	0.30	**124.6**	51.7	1.14	0.20	**-71.0**	61.7	1.02	0.14
"	0.30	**-8.3**	59.7	1.61	0.13	**-71.0**	42.7	1.51	0.12
50, Inner **surface**	/	**24.1**	21.3	1.53	0.14	**-16.7**	39.5	1.39	0.09
50, Inner **side**	0.05	**48.4**	9.0	1.52	0.08	**23.5**	37.4	1.49	0.08
"	0.10	**50.7**	29.6	1.59	0.18	**11.1**	39.5	1.42	0.15
"	0.20	**38.3**	48.2	1.35	0.13	**-16.0**	63.1	1.30	0.18
"	0.25	**-157.9**	40.8	1.43	0.21	**129.6**	25.6	1.48	0.30
"	0.30	**-31.7**	49.1	1.46	0.26	**150.0**	96.1	1.23	0.29
"	/	**-123.1**	16.9	1.5	0.28	**-57.7**	63.3	1.78	0.10

TABLE A1. (CONTINUED) RESIDUAL STRESS OBSERVED VIA XRD ON THE SMALL SAMPLE'S OUTER AND INNER SIDE: PROGRESSIVE ELECTROLYTIC REMOVAL

P22 pipeline's small sample		Stress-mesurement direction				Principal stress					
		90° (cylinder's longitudinal direction)									
Distance from the weld [mm], Location on the pipeline	Depth [mm]	**Stress** [Mpa]	Error (+-) [Mpa]	FWHM [°]	Error (+-) [°]	σ_1 [Mpa]	Error (+-) [Mpa]	σ_2 [Mpa]	Error (+-) [Mpa]	φ [°]	Error (+-) [°]
5, Outer **surface**	/	**351.6**	5.6	2.03	0.03	**376.1**	8.9	**344.0**	8.9	29.2	13.6
5, Outer **side**	0.10	**542.8**	141.0	1.27	0.34	**787.5**	109.4	**-13.7**	109.4	56.5	6.1
"	0.15	**163.4**	126.7	1.29	0.28	**418.5**	114.9	**138.4**	114.9	17.4	25.3
"	0.20	**266.6**	72.3	1.24	0.30	**275.0**	65.9	**67.8**	65.9	78.3	22.4
"	0.25	**186.7**	92.2	1.35	0.27	**228.2**	84.7	**92.3**	84.7	56.5	27.2
20, Outer **surface**	/	**110.5**	55.4	1.87	0.17	**270.9**	37.1	**88.8**	37.1	20.2	10.4
20, Outer **side**	0.10	**-72.6**	143.6	1.14	0.32	**345.7**	187.2	**245.0**	187.2	32.7	13.0
"	0.15	**-87.3**	93.0	1.21	0.20	**141.5**	89.3	**107.2**	89.3	16.4	30.3
"	0.20	**0.3**	95.0	1.09	0.22	**65.8**	114.1	**-11.7**	114.1	23.1	93.1
"	0.25	**129.2**	55.7	1.24	0.14	**257.1**	224.8	**-8.4**	224.8	46.0	9.4
50, Outer **surface**	/	**79.1**	43.7	1.72	0.25	**210.8**	48.0	**78.1**	48.0	4.9	27.2
50, Outer **side**	0.05	**-194.8**	86.0	1.38	0.25	**161.6**	73.4	**277.0**	73.4	25.7	9.0
"	0.10	**205.0**	125.9	1.47	0.19	**408.0**	97.2	**-24.2**	97.2	46.7	9.1
"	0.15	**111.9**	88.9	1.24	0.20	**181.5**	98.0	**138.9**	98.0	62.2	15.0
"	0.25	**-29.3**	68.3	1.33	0.19	**198.9**	121.9	**188.9**	121.9	39.9	12.5
"	0.30	**18.8**	169.7	1.08	0.30	**159.5**	148.4	**262.5**	148.4	54.7	14.9
"	0.35	**61.4**	30.7	1.12	0.21	**142.4**	113.3	**112.2**	113.3	55.7	15.9
"	0.40	**-153.3**	85.6	1.01	0.18	**-8.0**	93.1	**239.7**	93.1	37.6	16.2
5, Inner **surface**	/	**41.6**	58.0	1.47	0.17	**64.50**	40.3	**-37.8**	40.3	61.8	18.9
5, Inner **side**	0.05	**21.2**	32.4	1.17	0.09	**118.5**	54.1	**112.4**	54.1	49.5	7.1
"	0.10	**27.6**	43.6	1.18	0.18	**42.2**	48.7	**15.2**	48.7	42.6	58.3
"	0.20	**25.5**	30.5	1.25	0.19	**102.9**	44.0	**4.2**	44.0	27.7	22.8
"	0.30	**56.7**	53.5	1.31	0.22	**111.3**	52.5	**-26.0**	52.5	50.9	16.5
"	0.35	**26.8**	70.4	1.19	0.25	**133.2**	54.9	**145.8**	54.9	51.9	8.1
"	0.35	**-103.7**	37.3	1.63	0.10	**-99.3**	38.2	**141.6**	38.2	71.3	67.7
20, Inner **surface**	/	**-54.9**	56.4	1.35	0.27	**8.50**	63.2	**-64.2**	63.2	21.0	41.4
20, Inner **side**	0.05	**57.4**	16.6	1.43	0.16	**85.4**	27.7	**-30.4**	27.7	60.5	11.3
"	0.10	**-5.8**	20.4	1.49	0.09	**117.6**	24.7	**134.8**	24.7	45.6	3.6
"	0.20	**29.9**	53.5	1.22	0.21	**78.2**	52.1	**-7.5**	52.1	41.4	24.1
"	0.25	**51.2**	30.3	1.56	0.27	**141.9**	49.7	**-34.3**	49.7	44.1	10.3
"	0.30	**61.9**	57.0	1.55	0.30	**260.5**	63.7	**-74.0**	63.7	39.6	6.9
"	0.30	**-92.4**	26.5	1.61	0.21	**-3.5**	42.2	**-97.2**	42.2	13.1	30.8
50, Inner **surface**	/	**-11.6**	26.3	1.55	0.07	**35.30**	30.3	**-22.8**	30.3	26.0	29.2
50, Inner **side**	0.05	**18.7**	55.2	1.28	0.18	**51.5**	37.3	**15.6**	37.3	17.1	66.6
"	0.10	**62.5**	44.1	1.50	0.10	**102.4**	42.7	**10.7**	42.7	48.7	16.9
"	0.20	**100.6**	65.2	1.30	0.11	**160.4**	65.0	**-21.5**	65.0	55.0	14.5
"	0.25	**-0.2**	65.7	1.34	0.13	**144.0**	50.3	**302.0**	50.3	55.4	5.1
"	0.30	**119.0**	99.2	1.22	0.30	**174.0**	87.6	**-86.7**	87.6	62.7	17.2
"	/	**-205.9**	28.0	1.54	0.17	**-49.9**	46.3	**279.0**	46.3	34.4	7.0

ANNEX A CONTINUED

TABLE A2. RESIDUAL STRESS OBSERVED VIA XRD ON THE PIPELINE'S OUTER SURFACE (SAMPLES SMALL, 1, 2 AND 3) **[1]**

Sample	Distance from the weld [mm]	Stress-mesurement direction												Principal stress					
		0° (cylinder's tangential direction)				**45°**				**90°** (cylinder's longitudinal axis)									
		Stress [Mpa]	Error (+-) [Mpa]	FWHM [°]	Error (+-) [°]	**Stress** [Mpa]	Error (+-) [Mpa]	FWHM [°]	Error (+-) [°]	**Stress** [Mpa]	Error (+-) [Mpa]	FWHM [°]	Error (+-) [°]	σ_1 [Mpa]	Error (+-) [Mpa]	σ_2 [Mpa]	Error (+-) [Mpa]	φ [°]	Error (+-) [°]
Small	2.5	**434.4**	15.8	2.58	0.05	**349.0**	23.2	2.52	0.07	**188.0**	16.2	2.53	0.04	**440.1**	14.7	**182.4**	14.7	-8.5	5.5
1	5	**453.1**	21.3	2.57	0.09	**391.8**	6.9	2.55	0.10	**212.4**	10.0	2.63	0.07	**466.9**	14.6	**198.7**	14.6	-13.1	2.8
1	20	**404.8**	25.3	2.48	0.10	**310.9**	20.1	2.34	0.05	**160.7**	20.3	2.42	0.08	**408.1**	20.1	**157.5**	20.1	-6.5	5.8
2	5	**395.4**	14.1	2.40	0.08	**319.4**	19.3	2.36	0.06	**220.1**	13.6	2.31	0.11	**396.2**	12.1	**219.3**	12.1	-3.8	7.0
2	20	**341.4**	20.3	2.46	0.03	**199.6**	15.2	2.40	0.06	**64.8**	10.1	2.37	0.07	**341.4**	13.9	**64.7**	13.9	0.7	3.9
2	50	**295.1**	16.7	2.49	0.08	**182.4**	18.0	2.39	0.08	**122.3**	8.4	2.45	0.11	**299.1**	12.1	**118.3**	12.1	8.5	6.2
3	50	**245.9**	23.2	2.23	0.05	**118.4**	17.1	2.23	0.09	**89.4**	15.0	2.23	0.05	**260.1**	18.1	**75.2**	18.1	16.1	6.2
3	100	**302.3**	32.6	2.32	0.04	**293.4**	18.0	2.28	0.04	**267.7**	7.1	2.27	0.07	**304.2**	21.2	**265.8**	21.2	-13.0	34.6

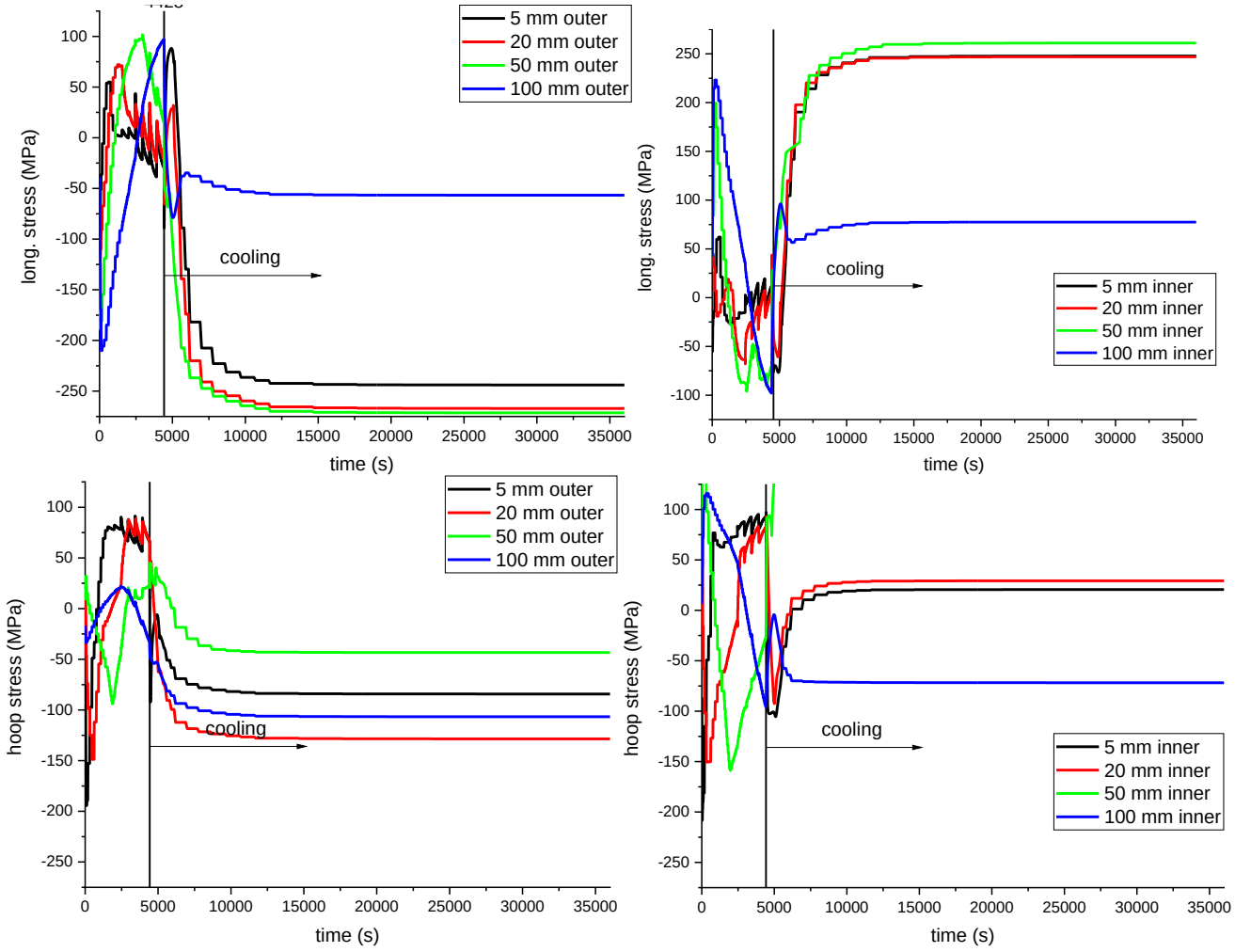

FIGURE A1. THERMAL ANALYSIS FOR THE BUTT JOINT: RESIDUAL STRESSES VS. TIME AT DIFFERENT LOCATIONS ON BOTH OUTER (LEFT) INNER SURFACES **[1]**

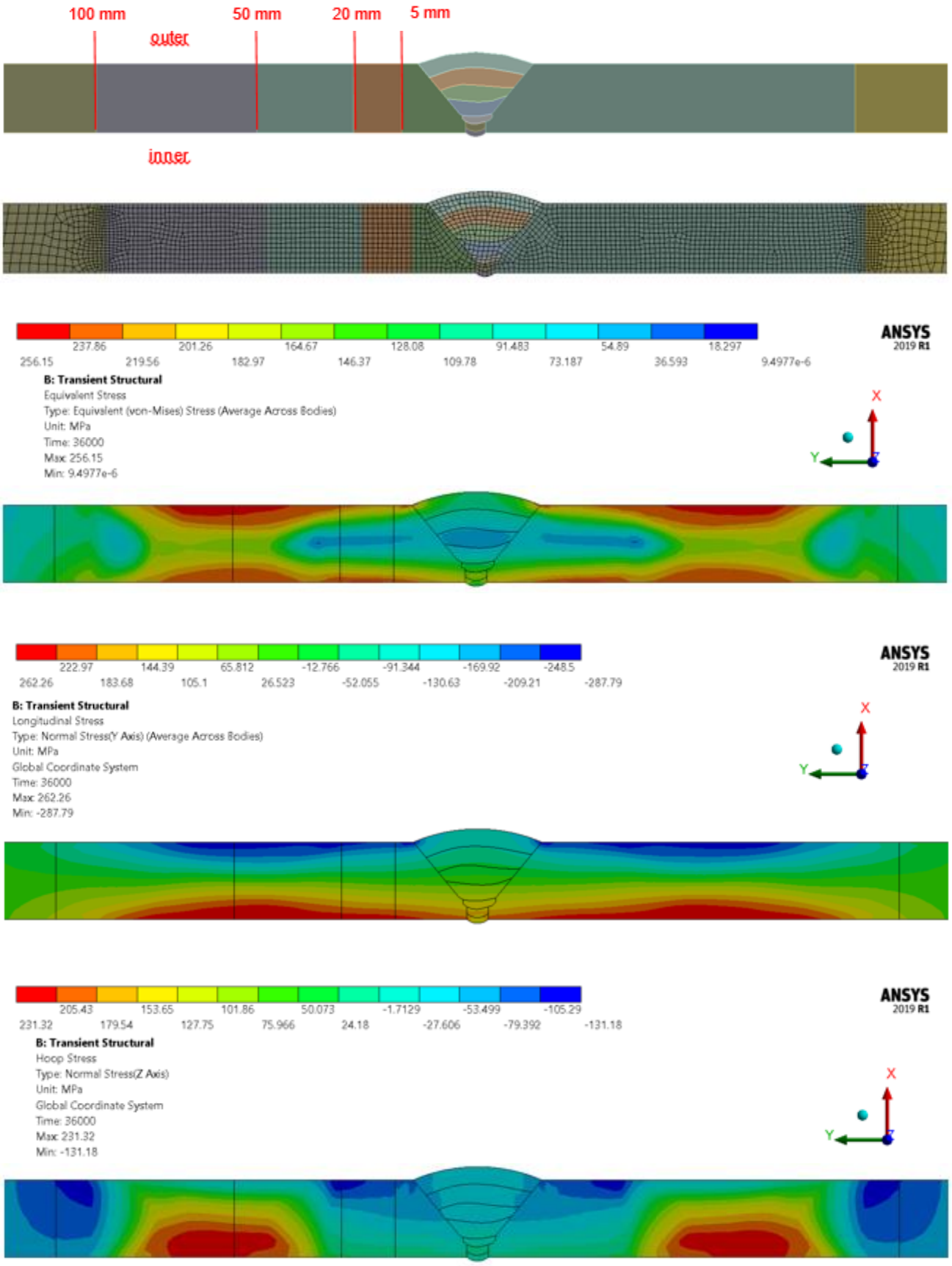

FIGURE A2. GEOMETRY (ABOVE), MESH, THERMAL ANALYSIS FOR THE BUTT JOINT: RESIDUAL STRESSES (FROM ABOVE EQUIVALENT, LONGITUDINAL, HOOP) AFTER 10 HOURS (COMPLETE WELD COOLING) **[1]**

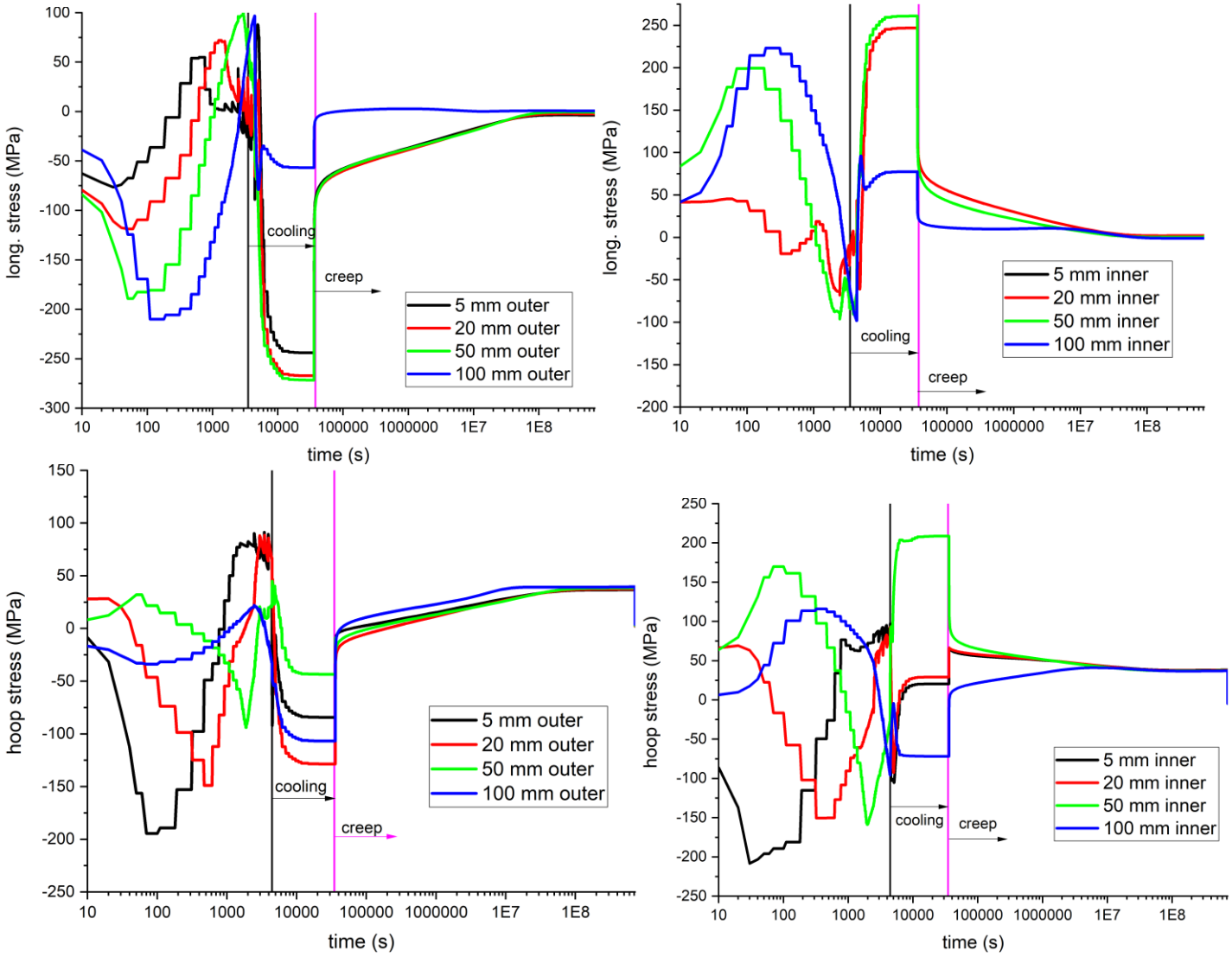

FIGURE A3. STRESSES ON BOTH OUTER (LEFT), INNER BUTT-JOINT SURFACES DURING WELDING (0-10 HOURS, VIRTUALLY) AND DURING OPERATION (10-200,000 HOURS): PRESSURE + THERMAL LOAD + RESIDUAL STRESS **[1]**

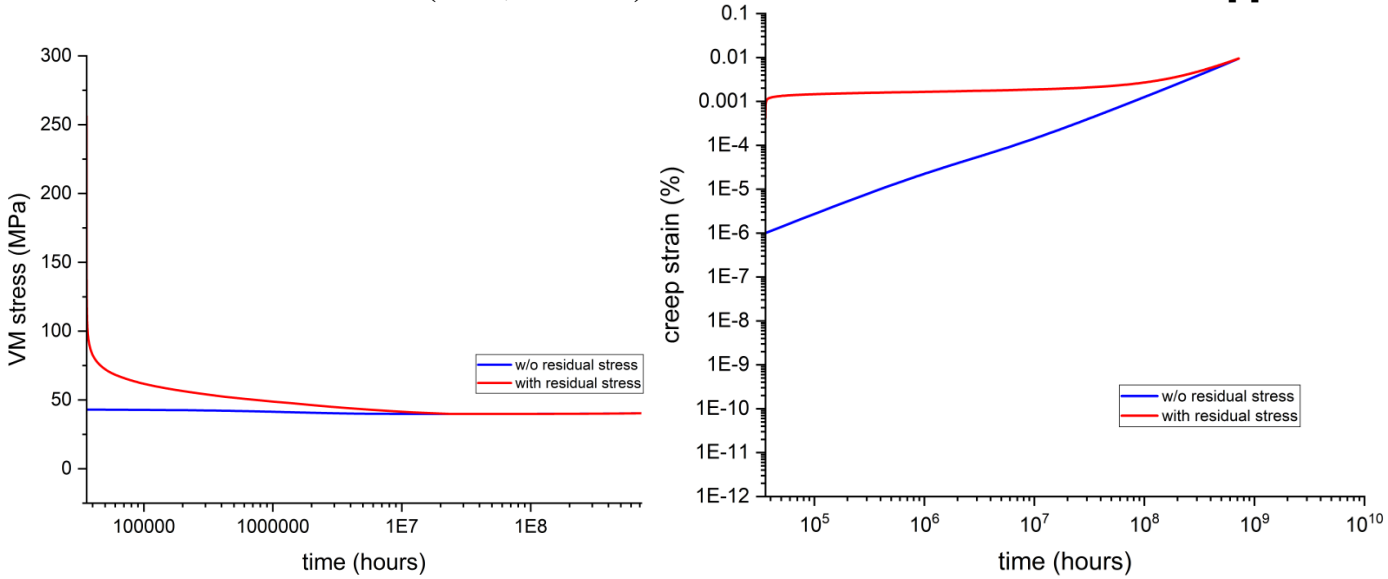

FIGURE A4. CREEP ANALYSIS WITH/WITHOUT RESIDUAL STRESSES: CASE FOR THE BUTT JOINT **[1]**

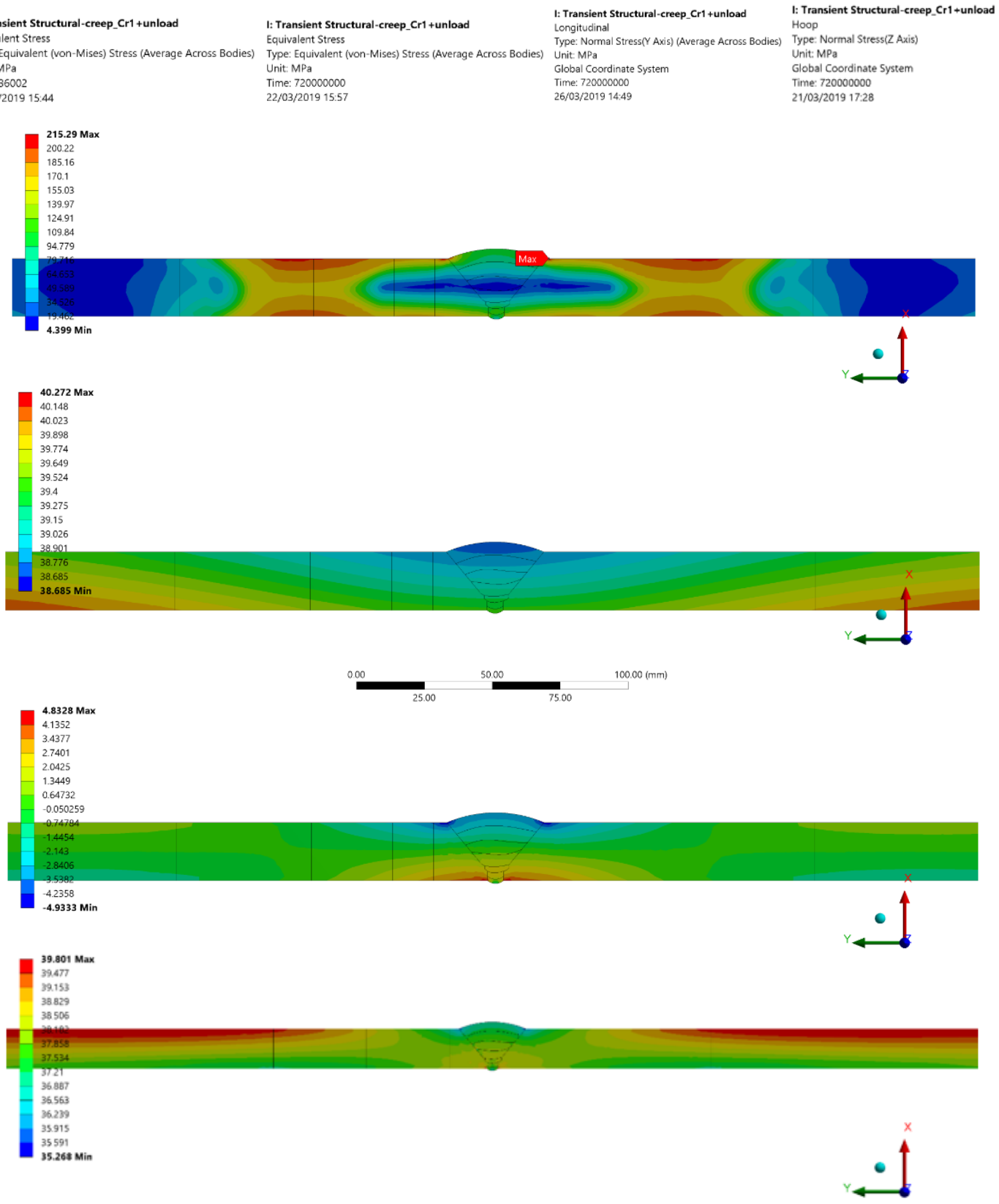

FIGURE A5. STRESS DISTRIBUTION (FROM ABOVE EQUIVALENT, LONGITUDINAL, HOOP) FOR THE BUTT JOINT AFTER 10 (ABOVE), 200,000 HOURS: CREEP-RELAXATION UNDER PRESSURE + THERMAL LOAD + RESIDUAL STRESS **[1]**